

On coupled mechanical harmonic oscillators, transients, and isolated oscillating systems

Lance McCarthy^{a)}

The Flinders University of South Australia, GPO Box 2100, Adelaide 5001, Australia

(Received 10 April 2001; accepted 27 November 2002)

Experimental results for the transient response of a single oscillator, for two magnetically coupled oscillators, and for oscillations about the center of mass of an isolated system are presented. The apparatus is easy to build. The data for the response and for the forcing term are acquired in a simple way, and allow accurate analysis and comparison with theory. © 2003 American Association of Physics Teachers.

[DOI: 10.1119/1.1539101]

I. INTRODUCTION

A flat steel spring with a mass m attached at one end and clamped to a massive support mass M at the other end provides a mechanical oscillator system in which the flat spring constrains the oscillations to remain in a plane, so that the displacement is well defined and expressed by a single variable. If one or more ceramic magnets are attached to the oscillating mass, a nearby small response coil can detect a time varying magnetic flux and give a measure of the velocity of the oscillating mass. A second coil fed by an alternating current and placed close to the ceramic magnets can be used to excite oscillations and will be referred to as the drive coil. The basic layout of such an oscillator system is shown in Fig. 1(a), and details given in Fig. 1(b). Eddy currents induced in a copper plate placed close to the magnet will cause damping.

This simple system can be built easily. Free and forced oscillations and transient behavior can be studied, with or without damping. If the support system mass M is reduced and arranged so that it can move freely, for example by suspending the whole system as a long pendulum, isolated oscillations in the center-of-mass system can be investigated. A pair of pendulums as shown in Fig. 2, that are coupled by a link, constitute a very useful apparatus for demonstrating the concepts of classical eigenmodes, eigenfrequencies and perturbation theory, but do not permit detailed experimental investigations. But if two flat springs, each with an attached mass and a magnet are clamped close together on a massive support, as shown in Fig. 3(a), with details given in Fig. 3(b), the interactions between the magnets couples these oscillators. Symmetric or antisymmetric classical eigenmodes of these coupled oscillators can be excited by the appropriate placement of the drive coil and orientation of the magnets. The eigenfrequency of the antisymmetric eigenmode can be studied as a function of the separation distance between the magnets. A drive coil and a response coil, as introduced above for the single flat spring oscillator, enable data collection and accurate experimental investigations of these magnetically coupled oscillators to be made.

A single oscillator system built with a flat steel spring, attached mass and magnet, with a velocity response coil and a drive coil to provide data, gives results for forced excitation and magnetic damping that are the same as those obtained with other systems.¹ However, setting up the single oscillator system with the drive and response coils is a useful first step for gaining experience for the later work on coupled oscillators and center-of-mass oscillators. So the experimen-

tal results for the transient response of single oscillator when a forcing excitation is suddenly applied are presented first as a simple example. The experimental techniques are then extended to more complicated systems.

II. EXPERIMENTS

A. Transient response of a single mechanical harmonic oscillator

The system was constructed with a single flat steel spring whose cross section was 1.5 mm × 32 mm; the length between the mass and clamp point was approximately 250 mm. The oscillating mass, including the magnets, was chosen to give a natural oscillation frequency about 8 Hz. Magnets of area 25 mm × 40 mm and thickness 10 mm were used. Two magnets mounted on the spring with a small gap between them can be useful. These two magnets permit a greater separation between the drive coil and the velocity response coil. The magnetic field also can be measured by placing a Hall probe in the gap. The magnetic interaction for the later coupling experiments can be modeled by considering coils of the same area as the magnets, carrying currents that make the same field at the center as measured by the Hall probe.

The rectangular velocity response coil consisted of 100 turns of 0.3-mm-diam wire supported by a 75-mm × 60-mm plastic frame. One of the 75-mm sides was placed in the region of the strong field of one magnet, parallel to the 40-mm dimension of the magnet. The plane of the coil is parallel to the plane of the face of the magnet. The response coil and the drive coil are shown in Figs. 1(a) and 1(b). The other 75-mm side of the response coil is in a region of very much lower field. With small oscillation amplitudes of ~3 mm, the flux change is mostly associated with sweeping the strong magnetic field past the side of the coil in the strong field region and is roughly (~3 mm × 40 mm) times B , where B is the magnitude of the strong magnetic field. The drive coil is slightly smaller, 70 mm × 45 mm, with 100 turns of 0.375-mm-diam copper wire, and is fed through a 3-Ω resistor from a signal generator and audio amplifier. This resistive load provides a signal for the data acquisition system, giving information on the forcing term. A personal computer with an analog-to-digital convertor is used to collect the data from both the drive and velocity response coils.

For these experiments the response signal was recorded and plotted using MATHCAD. A plot of the modeled behavior (see the following) can be compared to the experimental data

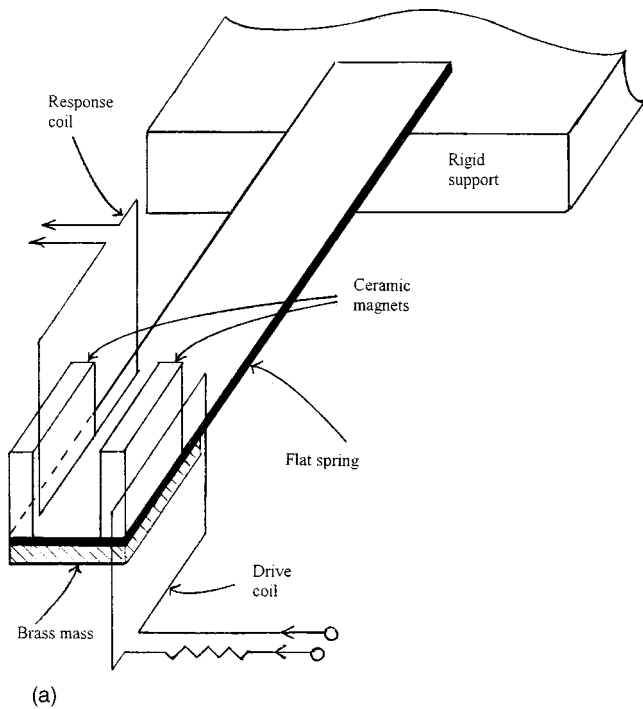


Fig. 1. General view of the flat spring harmonic oscillator. (b) End view of the flat spring harmonic oscillator showing the relation between the response coil, the drive coil, and the magnets.

on the same graph. The response frequency is one of the parameters that can be varied. Alternatively, the response frequency can be extracted using FFT in MATHCAD or by a separate package.

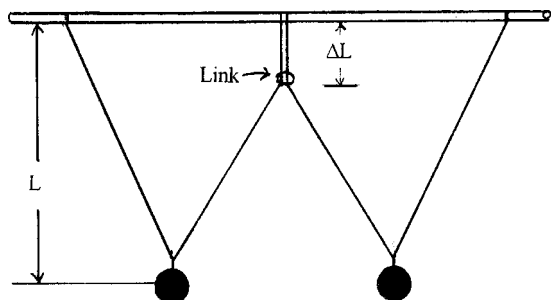


Fig. 2. A simple coupled harmonic oscillator system with coupling link.

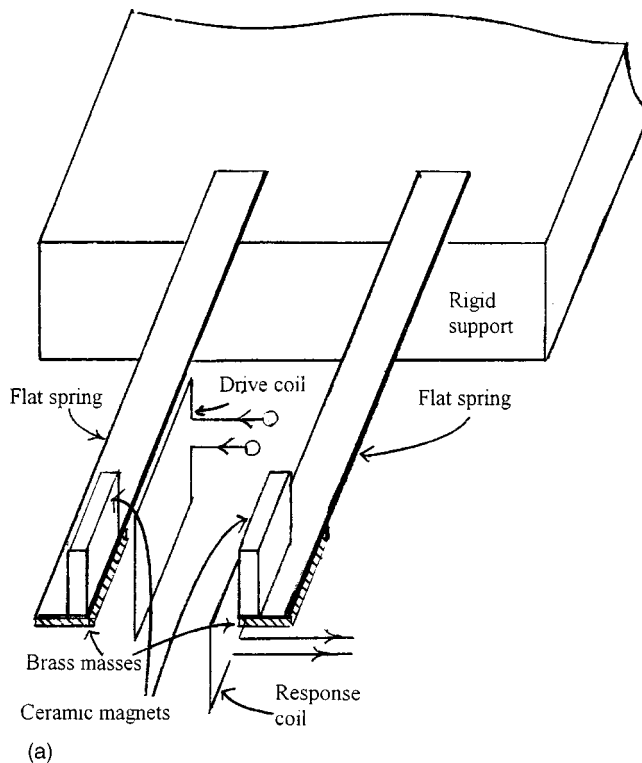


Fig. 3. (a) General view of the flat spring coupled harmonic oscillator system, showing the coupling magnets, response coil, and drive coil. (b) End view of the flat spring coupled harmonic oscillator system, showing the relation between the response coil, the drive coil, and the magnets. For this arrangement, with the drive coil located centrally and the magnets oriented with their magnetic moments anti-parallel, the antisymmetric eigenmode can be excited.

In the transient experiments, the natural resonant frequency, f_0 , of the oscillator is roughly determined first. The signal generator is then set to a frequency f close to but different from f_0 . Then the analog-to-digital convertor is set to receive the drive and response signals, and the audio amplifier is immediately switched on so that the oscillating driving force of amplitude F goes from zero to $F \cos(2\pi ft - \phi)$. The sudden switch-on means that the driving force is a product of a step function and a sinusoidal driving term. Because the step function is nonperiodic, its spectrum has a continuous range of frequencies that includes the resonant frequency. Alternatively, we could consider the step function alone to behave like a displacement from equilibrium causing a natural oscillation, decaying on a time scale determined

by the Q of the system. These oscillations will beat with those forced at frequency f , until the natural oscillations die away.

The equation of motion for the system can be written as

$$\frac{d^2x}{dt^2} + \frac{b}{m} \frac{dx}{dt} + \frac{k}{m}x = \frac{F}{m} \cos \omega t, \quad (1)$$

where the coefficient b is real. The form of the damping term is appropriate for the case of a high Q system with residual air and internal friction damping, and no added electromagnetic damping; k is the spring constant, m is the mass, and F and $\omega = 2\pi f$ are the amplitude and angular frequency of the forcing term. The solution of Eq. (1) can be written as:

$$x_1(t) = x_{10} \cos(\omega t - \phi_1). \quad (2)$$

Equation (2) is the usual form of the solution for a forced damped harmonic oscillator in the steady state. This solution is the particular integral, but the sudden switch on of the forcing term tells us that we must also include the solution to

$$\frac{d^2x}{dt^2} + \frac{b}{m} \frac{dx}{dt} + \frac{k}{m}x = 0. \quad (3)$$

The solution to Eq. (3) is the complimentary function:

$$x_2(t) = x_{20} e^{-\gamma t} \cos(\omega_0 t - \phi_2), \quad (4)$$

where

$$\gamma = \frac{b}{m} \quad (5)$$

is the decay rate of the natural oscillations whose angular frequency is ω_0 , and

$$\omega_0^2 = \frac{k}{m}. \quad (6)$$

The complete solution is then

$$\begin{aligned} x(t) &= x_1(t) + x_2(t) \\ &= x_{10} \cos(\omega t - \phi_1) + x_{20} e^{-\gamma t} \cos(\omega_0 t - \phi_2). \end{aligned} \quad (7)$$

The corresponding velocity is the time derivative of $x(t)$ in Eq. (7):

$$\begin{aligned} v(t) &= -x_{10} \omega \sin(\omega t - \phi_1) - x_{20} e^{-\gamma t} [\gamma \cos(\omega_0 t - \phi_2) \\ &\quad + \omega_0 \sin(\omega_0 t - \phi_2)]. \end{aligned} \quad (8)$$

The procedure is to display the experimental record of the velocity over a time interval long compared to the decay time, and fit the data to Eq. (8) by varying the parameters such as the phases, frequencies, forcing term strength, decay rate, as detailed in Fig. 4. The sudden switch-on suggests that the amplitudes x_{10} and x_{20} will be equal. The fit shown in Fig. 4 demonstrates that the observations were consistent with the theoretical predictions of transients at the natural frequency beating with the forced oscillations as they decay. The frequencies were extracted from the fitting procedure, and the frequency for the forcing term confirmed by comparison with the value set on the signal generator.

B. Harmonic oscillations of systems in the center-of-mass frame

The number of classical mechanical phenomena that can be readily observed and whose analysis in the center-of-mass

frame greatly aids the understanding is not large. The most well known and frequently made observations of this kind are of the tides. If tides are considered in the reference frame where the earth and moon are rotating about their common center of mass, it is easily seen that the distribution of the earth's water envelope produces two lunar tides per day, see for example, Brown,² or Rogers.³ In other reference frames the explanation is more difficult. It is useful for pedagogical purposes to consider laboratory experiments and demonstrations that demand analysis in the center-of-mass reference frame.

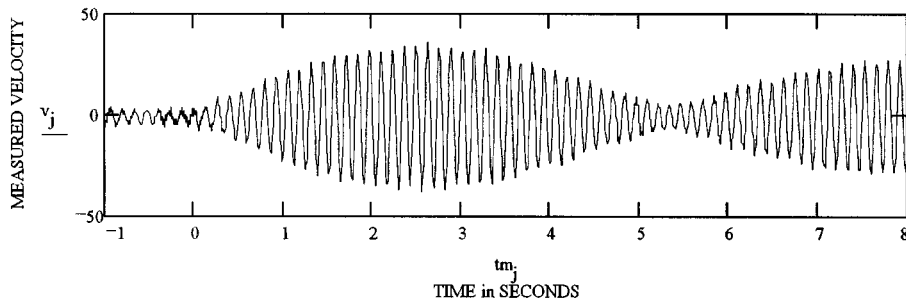
In developing accurate experiments on the simple harmonic oscillator,¹ the problem of using a finite mass support rather than a completely rigid support became obvious. A 171-kg optical table was used as the support, and when a relatively small mass was left on the table by mistake, a lower resonant frequency was obtained. This observation was followed up by measuring the resonant frequency for a sequence of mass increments. The data showed that the resonant frequency for this system on the optical table decreased from 10.7799 Hz for a base mass of 171 kg to 10.7569 Hz for 271 kg. These observations suggest that the support mass be deliberately changed in order to develop a demonstration experiment for which the analysis must be done in the center-of-mass frame.

For this experiment, flat springs, plus an effective oscillator mass of m including the attached magnets are clamped to a frame of finite mass M that includes the drive and detector coils; M can be increased by attaching other masses to the frame, as shown in Fig. 5. The complete system is suspended as a pendulum of length ~ 2.5 m, and the oscillations are arranged to take place in the horizontal plane. Suspending the system in this way allows the small amplitude oscillations of both m and M to take place almost isolated from other effects. The oscillations of this system must be considered in the center-of-mass frame.

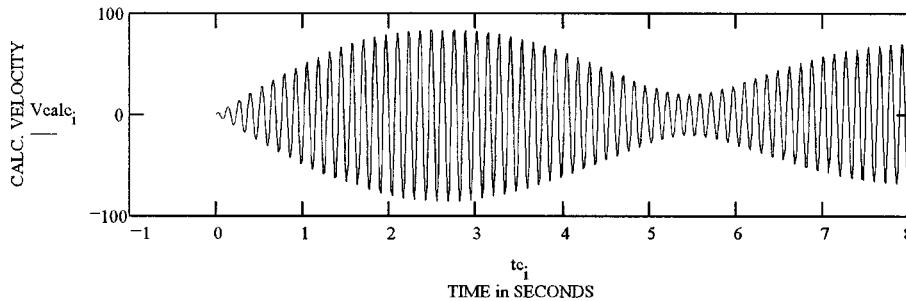
When M is incremented by amounts ΔM_i , the resonant frequency decreases. The design of such a system has to ensure that for all choices of ΔM_i , the center-of-mass and the pendulum attachment point remain in the plane of the oscillations. A single flat spring and attached mass m clamped to one end of the frame results in angular as well as linear oscillations. To avoid the problem of angular oscillations and ensure that only linear oscillations occur, a symmetrical system as shown in Fig. 5 was made using a piece of aluminum channel as the frame for the base of mass M . Two identical flat springs were clamped to opposite ends of the frame, each having an attached mass $m/2$ located close to the center of mass. Each mass had a magnet attached, whose principal purpose was providing the velocity response signal. These magnets were placed very close together and oriented so that they attract each other, ensuring that the masses move together. This part of the system thus acts as a single oscillator with total oscillating mass m , and a combined spring constant k .

To predict the behavior of the system, we take x to be the coordinate of the mass m , and X to be the coordinate of the frame with mass $M + \Delta M_i$, each measured with respect to the center of mass. Conservation of momentum requires that the velocities be opposite at all times and hence the displacement of the spring is the sum of the displacements of m and $M + \Delta M_i$. We apply a sinusoidally varying forcing term us-

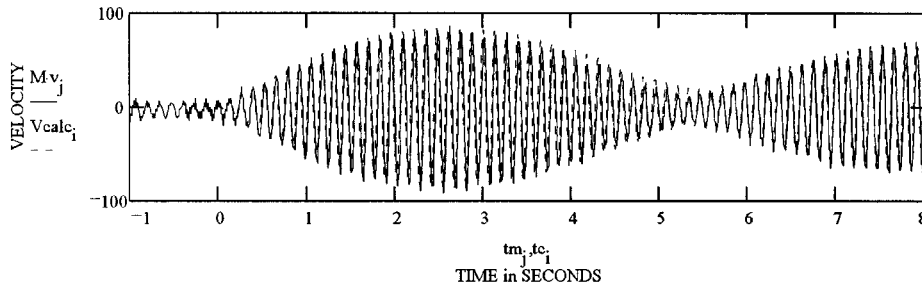
(a) The experimental data consisting of 4096 samples of the transient velocity signal v , taken at 10ms intervals are read into a file v , and some of this data is plotted to show the general behaviour :



(b) Next, a velocity V is calculated each 10ms using Eq 8. Unit amplitudes are used. The frequencies f , f_0 , phases ϕ , ϕ_0 , and decay rate γ can be varied.



(c) The calculated velocity is plotted over the experimental data. The frequencies f , f_0 , the phases ϕ , ϕ_0 , the decay rate γ and signal strength (using the multiple M) are all varied manually to obtain the best fit as judged by eye. A general view of data and fit :



Details are shown :

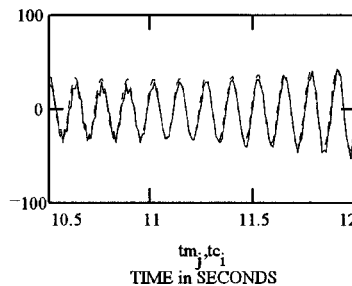
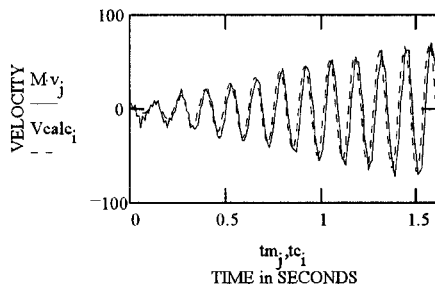


Fig. 4. Data and calculations for investigations of transient oscillations. (a) The experimental data. (b) Information about the process of making theoretical calculations for the comparison. (c) Information on the comparison of experimental data with theoretical calculations.

ing a magnet mounted as part of m , interacting with a coil carrying an ac current mounted as part of $M + \Delta M_i$. The equations of motion for the individual masses may then be written as:

$$\frac{d^2x}{dt^2} + \frac{b}{m} \frac{d(x+X)}{dt} + \frac{k}{m}(x+X) = \frac{F_0}{m} \cos \omega t. \quad (9)$$

$$\frac{d^2X}{dt^2} + \frac{b}{M + \Delta M_i} \frac{d(x+X)}{dt} + \frac{k}{M + \Delta M_i}(x+X) = \frac{F_0}{M + \Delta M_i} \cos \omega t. \quad (10)$$

If we combine Eqs. (9) and (10), we can write:

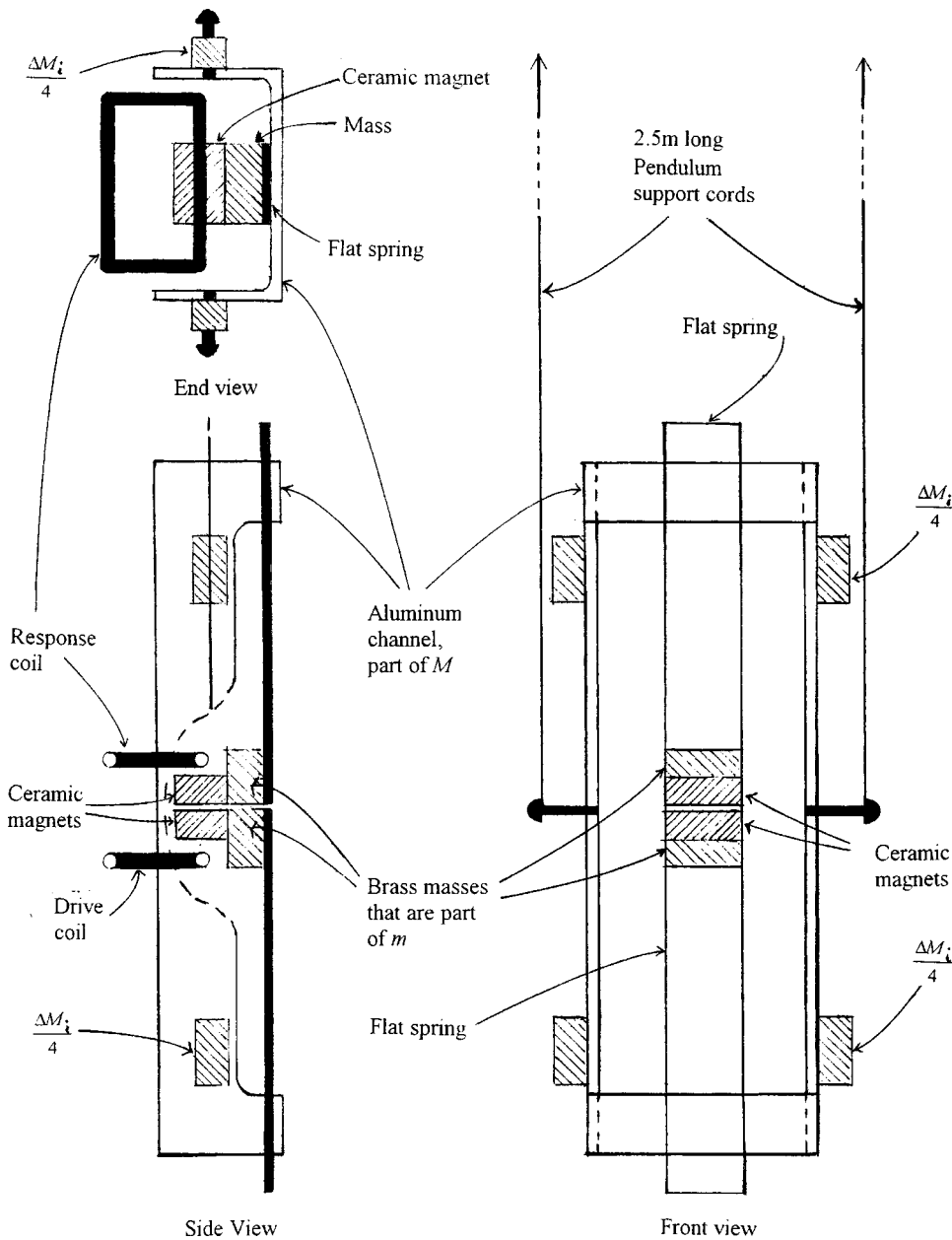


Fig. 5. Basic diagram of a center-of-mass oscillator system.

$$\frac{d^2(x+X)}{dt^2} + \frac{b}{M_r} \frac{d(x+X)}{dt} + \frac{k}{M_r} (x+X) = \frac{F_0}{M_r} \cos \omega t, \quad (11)$$

where the reduced mass is

$$M_r(\Delta M_i) = \frac{m(M + \Delta M_i)}{m + M + \Delta M_i}. \quad (12)$$

Equation (11) has the same form as the equation for a forced simple harmonic oscillator with the reduced mass M_r moving relative to a rigid support. Such a system is characterized by a resonant angular frequency ω_0 , which depends on the increment ΔM_i :

$$\begin{aligned} \omega_0^2(\Delta M_i) &= \frac{k}{M_r} = \frac{k(m + M + \Delta M_i)}{m(M + \Delta M_i)} \\ &= \frac{k}{m} \left(1 + \frac{m}{M + \Delta M_i} \right), \end{aligned} \quad (13)$$

where $\omega_0(\Delta M_i)$ is the resonant angular frequency for the base mass $M + \Delta M_i$.

For these experiments M was about $3m$, so that $\omega_0(\Delta M_i)$ can be made to decrease by about 15% as ΔM_i is increased from zero to very large values. The oscillating mass m and mass of the base M were measured using a laboratory balance. They were found to be $m \sim 0.65$ kg and $M \sim 2.1$ kg. Static measures of the spring constant gave $k \sim 1425$ N m⁻¹. The oscillating mass m is not just that of the masses attached to the spring, but includes some of the spring mass. The effective oscillating mass, which is the quantity that m represents, can be determined in an auxiliary experiment where the frame M is clamped to a very massive support and m is varied by amounts δm_i . Then

$$\omega_0^2(\delta m_i) = \frac{k}{m + \delta m_i}. \quad (14)$$

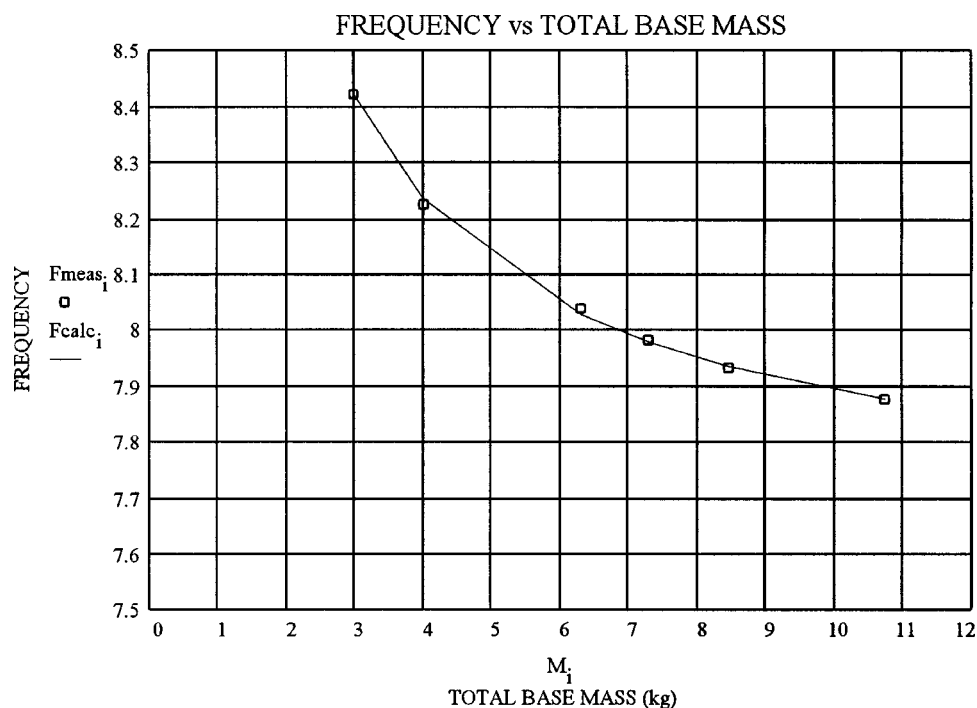


Fig. 6. Comparison of experimental data with theory, for center-of-mass oscillations when the base mass is incremented. The experimental data are shown as boxes. The solid line is the theoretical fit obtained when the parameters k , m , and the minimum base mass M , have been varied to obtain the best fit. The values of these parameters that give the best fit were found to be $k=1452.8 \text{ Nm}^{-1}$, $m=0.628 \text{ kg}$, and $M=2.04 \text{ kg}$, consistent with the roughly measured values noted in the text.

A comparison of a plot of $k/\omega_0^2(\delta m_i)$ vs δm_i with a plot of $m + \delta m_i$ vs δm_i can be used to determine the effective spring constant k and oscillating mass m . This determination is not presented, because the quantities k and m are not the main interest and their values can be obtained from measurements on the isolated system.

The resonant frequency for the isolated system can be extracted, for example, by initiating a transient and taking the FFT of the velocity trace. Data for $f_0(\Delta M_i)$ are taken for a range of values of ΔM_i as this increment of mass is increased, keeping the increment symmetrical about the center of mass. Equation (13) can be written in terms of the frequency

$$f_0(\Delta M_i) = \frac{1}{2\pi} \sqrt{k \frac{m + M + \Delta M_i}{m(M + \Delta M_i)}}. \quad (13')$$

Figure 6 displays the experimentally measured $f_0(\Delta M_i)$ vs $M + \Delta M_i$ for this isolated system. The data were fitted using Eq. (13') by varying the values of k , m , and M . The best fit is shown as a solid line. The manual fitting process, judged by eye, is reasonably sensitive. For example, if m is changed from 0.628 kg, the value found to give the best fit, by half a percent to 0.625 kg a very noticeable misfit occurs.

These experiments model linear vibrations of molecules. The case of the system isolated on the pendulum is analogous to the stretching vibrations of a diatomic molecule in the gas phase. Textbooks on the applications of infrared spectroscopy to organic chemistry, for example, Refs. 4 and 5, discuss the stretching vibrations of diatomic molecules by calculating the vibrational frequency as a ball and spring system using the reduced mass. However, when discussing the factors influencing vibrational frequencies, they do not discuss the details of modeling the changes expected in going from the gas phase to the solid phase. When the frame is clamped to a rigid support, this oscillator system is analogous to a molecule in the solid. A reduction of the frequency

for infrared absorption in the solid state compared with that in gas phase would be expected, but no direct comparison has been found in the literature.

C. Coupled mechanical harmonic oscillators

A simple demonstration of coupled mechanical harmonic oscillators can be made using a pair of identical pendulums whose masses are a distance L below a common support, each constrained to have just one degree of freedom by using a pair of cords attached to a rod as shown in Fig. 2. The coupling strength of the pendulums can be varied using a sliding link connecting the adjacent cords as shown in Fig. 2. This simple apparatus permits an elegant demonstration of classical eigenmodes and eigenfrequencies. The frequency of the antisymmetric eigenmode when the link is ΔL below the support is approximately that of a pendulum of length $(L - \Delta L/2)$. The change of the eigenfrequencies of the two modes that are degenerate when $\Delta L=0$ can be considered as a function of ΔL . This apparatus does not lend itself to accurate measurements, because it is not simple to quantify the strength of the coupling through the link, and it is not easy to force the oscillations.

A pair of flat springs with attached masses and magnets as shown in Figs. 3(a) and 3(b) together with the exciter and detector coils and a rigid support system enables the coupled mechanical oscillator system to be investigated quantitatively as a function of the strength of the magnetic coupling. The strength of the magnetic coupling can be decreased by increasing the separation between the individual oscillators. By a suitable orientation of magnetic moments and drive coils, each of the eigenmodes can be excited and resonances observed. For free oscillations, the FFT of the response signal demonstrates that there is a mixture of the two eigenmodes. This FFT is used to extract the eigenfrequencies.

Coupled mechanical oscillators are discussed in books on vibration control such as Ref. 6, but the emphasis of these

books is on finding solutions of engineering problems. Symon discusses theoretical techniques for analyzing coupled systems,⁷ and suggests techniques for coupling including springs and friction. He gives a detailed theoretical analysis of systems coupled by a spring. Symon presents some examples of coupled oscillator vibration traces, but the data are not analyzed or compared with theory. It is not obvious how the strength of the coupling spring can be easily changed in a way that maintains the natural frequencies of the individual oscillators, because some fraction of the spring mass always contributes to the oscillator mass.

The strength of the magnetic coupling used in the experiments discussed in the following can be varied without changing the individual spring constants, or changing the individual oscillator masses. The natural frequencies of the individual oscillators are therefore maintained. The magnetic coupling can be quantified and varied in a well-defined way. The rigidity of the flat spring plus mass system ensures that the magnetic coupling does not alter the geometry of the path of the individual oscillations, as would occur for magnetically coupled, freely suspended pendulums, even with double cords as shown in Fig. 2.

Before we can write the equations of motion governing the coupled systems, we need to be able to represent the coupling term as a function of separation distance, and as a function of the relative displacement of the two oscillators. This term can be modeled by representing the magnets by dc current carrying single turn loops of radius a of equivalent area and magnetic moment. A Hall probe placed on the surface of the magnet was used to measure the B field that single turn loops with the same area as the magnets must match for the model. The value obtained was 0.12 T.

In modeling the interaction we regard one of the single turn loops as the source of a magnetic field. The current in the other loop was regarded as the response loop and interacts with this field to produce the magnetic coupling term. Because the current stays fixed as we vary the separation z and the relative displacement x , we can find the dependence of the coupling term on z and x by calculating B as a function of these variables. To obtain the appropriate strength of the coupling, the oscillators must be placed so that the magnets or loops are separated by a distance that is the order of their linear dimensions. For this reason we need to calculate near-fields accurately at a range of locations.

An important point of this paper is that the vector potential \mathbf{A} has become valuable now that mathematical packages are readily available. Not only is it important to improve students' understanding of the vector potential,⁸ there is much to be gained by using \mathbf{A} for magnetic field calculations. Before the introduction of mathematical packages, the use of \mathbf{A} was difficult and even in graduate textbooks on electromagnetism,⁹ most problems involved approximations for far fields or on the fields near the axis of a current carrying coil. But by using mathematical packages, it is easy to calculate \mathbf{B} from the curl of \mathbf{A} everywhere, especially when \mathbf{A} is produced by circular current loops.

For the present case it is easiest to work in cylindrical coordinates (r, ϕ, z) , where the z axis lies along the undisplaced axes of the loops. The vector potential in these coordinates has only a ϕ component, and the interacting current also has only a ϕ component. The relative oscillatory displacement x increases the radial distance between one side of the response loop and the center of the source loop, and

decreases it on the other. The currents on opposite sides of the responding loop produce forces that are opposed. We need to find the behavior of $B_z(a+x, z)$ and $B_z(a-x, z)$ as a function of the displacement x and the separation z between the loops. We write the vector potential as:

$$A_\phi(r, z) = \frac{\mu_0 I a}{4\pi} \int_0^{2\pi} \frac{\cos \phi}{(a+r+z-2ar \cos \phi)^{1/2}} d\phi. \quad (15)$$

Then the z component of the \mathbf{B} field is obtained by taking the curl:

$$B_z(r, z) = \frac{1}{r} \frac{\partial}{\partial r} (r A_\phi(r, z)). \quad (16)$$

The estimate of the perturbing force is then

$$I[B_z(a+x, z) - B_z(a-x, z)]b, \quad (17)$$

where b is the effective length of the current perpendicular to both x and z . The value of b is chosen to be the length of the long side of the actual magnet.

The principles and results of the modeling of the spatial variation of this perturbing force are presented in Fig. 7. There are notes to guide readers to do the calculations in any mathematical package they prefer. The calculations have been done here using MATHCAD, but not all the details are shown; for example, it is necessary to calculate the interaction force using Bz . It is seen that the perturbation is proportional to the displacement x for a given value of the separation z , and proportional to z^{-4} for a given value of x . There is of course no relative displacement for the symmetric eigenmode, and so the magnetic coupling does not perturb the symmetric eigenfrequency. For the free, undamped asymmetric eigenmode, there is a term containing the spring constant k and a term containing a new quantity p defined as the perturbation force per unit displacement of the oscillator. For the opposed magnetic moment orientation chosen here, p provides a force in the opposite direction to that of the spring, and we write the equation of motion for each oscillator as:

$$\frac{d^2x}{dt^2} + \left(\frac{k}{m} - \frac{p}{m} \right) x = 0. \quad (18)$$

The solution to Eq. (18) is

$$x_1(t) = x_{10} \cos(\omega_{0A} t), \quad (19)$$

where for this antisymmetric eigenmode

$$\omega_{0A}^2 = \frac{k}{m} \left(1 - \frac{p}{k} \right). \quad (20)$$

For the symmetric eigenmode:

$$\omega_{0S}^2 = \frac{k}{m}. \quad (21)$$

The perturbation to the antisymmetric eigenfrequency in terms of the symmetric eigenfrequency for small perturbations is then approximately:

$$f_{0S} - f_{0A} = \frac{p}{2k} f_{0S}, \quad (22)$$

or in terms of angular frequencies:

$$\omega_{0S} - \omega_{0A} = \frac{p}{2k} \omega_{0S}. \quad (22')$$

(a) Define: $\mu_0 = 4 \cdot \pi \cdot 10^{-7}$ $I = 3.4 \cdot 10^3$ $a = 0.01784$

Use (Curl A)_z to calculate B_z:
$$B_z(r, z) := \frac{1}{r} \frac{d}{dr} \left[r \int_0^{2\pi} \frac{\mu_0 \cdot I \cdot a \cos(\phi)}{4 \cdot \pi \left(a^2 + r^2 + z^2 - 2 \cdot a \cdot r \cdot \cos(\phi) \right)^{\frac{3}{2}}} d\phi \right]$$

Examples :

1. B_z at r = 0.05mm, z = 0mm, very near the coil center : B_z(0.00005, 0.) = 0.119748

This can be checked with the 1st year Eq : $B = \frac{\mu_0 \cdot I}{2 \cdot a} = 0.119747$

2. B_z at the conductor of the other coil when the separation z = 50mm,

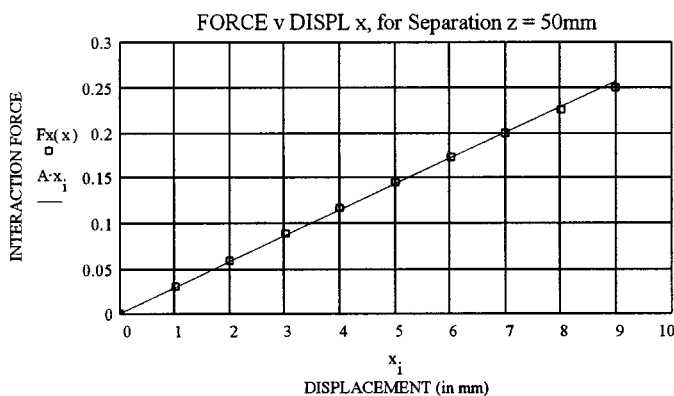
i. for relative displacement x = 0mm : B_z(a, 0.050) = 0.003409

ii. for relative displacement x = 2mm : B_z(a + 0.002, 0.050) = 0.003189

B_z(a - 0.002, 0.050) = 0.003621

Then calculate the interaction force as a function of displacement x, and separation distance z.

(b)



(c)

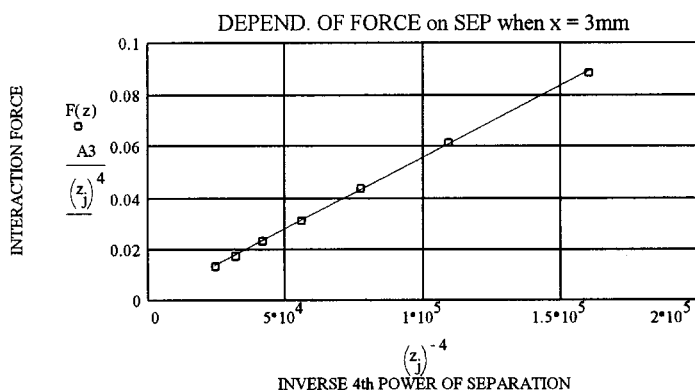


Fig. 7. (a) The basics of the calculations of the z component of B, used for modeling the interactions between the coupling magnets. The interaction force is the product of the current, the current element length, and the difference between the values of the B field at locations such as those calculated for relative displacement of 2 mm. The current element lengths are chosen in this modeling to be 40 mm, the actual length of the magnets. In (b) the interaction force $F_x(x)$ is plotted as a function of the relative displacement of the magnets, for the case when the separation distance is 50 mm. The calculated results are shown as boxes. Drawing the line Ax vs x , and varying the multiplier A to get the best fit shows that the dependence of $F_x(x)$ on x is linear. In (c) shown as boxes is the plot of the dependence of the interaction force $F(z)$ on the separation distance, for the case when the relative displacement is 3 mm. That the interaction is dependent on the inverse fourth power of the separation distance is shown, again by fitting a straight line, this time by varying the multiplier A^3 .

The spring constant was measured and found to be $k = 220 \text{ N m}^{-1}$. The symmetric eigenfrequency was measured to be $f_{0S} = 3.671 \text{ Hz}$, by taking a full resonance curve. For 50 mm separation and 5 mm displacement, our estimate for p is $p = 29 \text{ N m}^{-1}$. The predicted value of the antisymmetric eigenfrequency is then $f_{0A} = 3.43 \text{ Hz}$.

For interest and simplicity the data have been collected for the transient mixed mode excited when one oscillator is pulled aside and released. Alternately one oscillator can be struck gently. The data and analysis are presented in Fig. 8.

The two eigenfrequencies were then extracted using a FFT for different values of the separation distance z . With 4096 samples at 10 ms intervals, the FFT cannot determine frequencies to better than 0.025 Hz. Even so, the data and analysis confirm that the difference in the eigenfrequencies increases from zero at large separation as z^{-4} .

III. DISCUSSION AND CONCLUSIONS

The description of the apparatus, the presentation of typical data obtainable with this apparatus, and the data interpre-

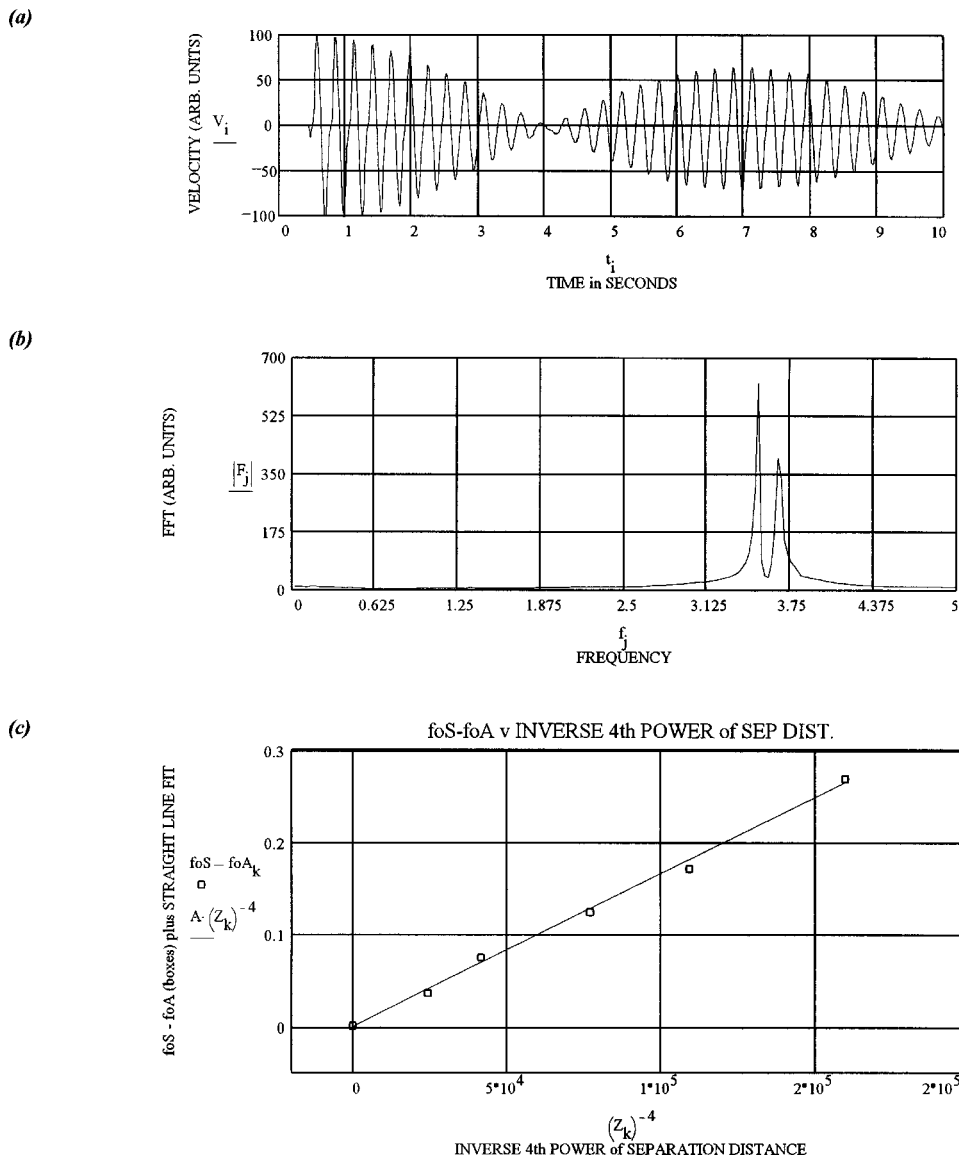


Fig. 8. In (a) is displayed a typical velocity trace for one of the coupled oscillators. For this case the separation between the magnets was 55 mm. (b) The FFT of the velocity trace from which the symmetric and antisymmetric eigenfrequencies f_{0S} and f_{0A} are determined. (c) shows as boxes the dependence of the difference between these eigenfrequencies ($f_{0S}-f_{0A}$) on the inverse 4th power of the separation distance z . The solid line labeled $A(Zk)^{-4}$ enables the linear relationship to be determined. A is the multiplier that is varied to obtain the best fit.

tation are intended as a guide to help interested readers construct simple harmonic oscillator systems for demonstrations and teaching laboratory experiments. Figures 4, 6, 7, and 8 demonstrate the ease with which the data can be analyzed and compared with theory.

Attention is drawn to the use of the vector potential when modeling the dependence of the perturbation on the separation and relative displacement of the coupling magnets presented in Fig. 7. Mathematical computer packages enable the vector potential to be used easily to calculate the magnetic fields everywhere. The near fields are obtained here with sufficient accuracy that their differences can be used to accurately model the experiment. Many laboratory coils are circular, and the vector potential in cylindrical coordinates, Eq. (15), is very useful.

⁰Electronic mail: lance.mccarthy@flinders.edu.au

¹L. McCarthy, "On the electromagnetically damped mechanical harmonic oscillator," *Am. J. Phys.* **64** (7), 885–891 (1996).

²Hanbury Brown, *Man and the Stars* (Oxford U.P., Oxford, 1978), p. 78.

³E. M. Rogers, *Physics for the Inquiring Mind* (Princeton U.P., Princeton, NJ, 1960), p. 328.

⁴J. C. D. Brand and G. Eglinton, *Applications of Spectroscopy to Organic Chemistry* (Oldbourne, London, 1965), pp. 23–24.

⁵W. Kemp, *Organic Spectroscopy* (Wiley, New York, 1975), pp. 14–17.

⁶W. J. Palm, *Modeling, Analysis and Control of Dynamic Systems* (Wiley, New York, 2001), 2nd ed., pp. 469–474.

⁷K. R. Symon, *Mechanics* (Addison–Wesley, Reading, MA, 1971), 3rd ed., pp. 191–201.

⁸M. D. Semon and J. R. Taylor, "Thoughts on the magnetic vector potential," *Am. J. Phys.* **64** (11), 1361–1369 (1996).

⁹J. D. Jackson, *Classical Electrodynamics* (Wiley, New York, 1975), 2nd ed., pp. 177–180.